Investigation of Phosphorus Site Condensation in $CaHPO_4$ by Analysis of ^{31}P MAS-NMR Tensor and X-Ray Powder Patterns

Faouzi Hlel, Saber Kamoun, and Kamel Guidara

Laboratoire de l'état solide, Faculté des Sciences de Sfax, B. P. 802, 3018 Sfax, Tunisia

Reprint requests to Dr. F. H.; E-mail: faouzihlel@yahoo.fr

Z. Naturforsch. **61a,** 375 – 382 (2006); received June 8, 2006

$CaHPO_4$ was obtained by slow evaporation at room temperature. Seven samples, obtained at different annealing temperatures, were characterized by X-ray diffraction and ^{31}P MAS-NMR spectroscopy. All NMR spectra were analyzed using a DMFIT program. At room temperature, the observed ^{31}P NMR chemical shifts for the title compound were -1.59, -0.36 and 1.26 ppm with the relative intensities 39%, 10% and 51%, revealing the presence of three non-equivalent phosphorus sites in the structure. The investigation of the NMR tensor shift of all spectra shows that the abounding HPO_4^{2-} anion was progressively transformed into $P_2O_7^{4-}$ when the temperature increased.

Key words: ^{31}P MAS-NMR Spectroscopy; Chemical Shift Tensor; $CaHPO_4$.

1. Introduction

Great attention has always been devoted to hydrogen phosphates of alkaline-earth metals like brushite ($CaHPO_4 \cdot 2H_2O$), monetite ($CaHPO_4$), $SrHPO_4$ [1 – 3]. These compounds are used in protonic conductors, batteries, fuel cells, etc. $CaHPO_4$ is found in bones and teeth; it also has practical uses in dental cements and restorative materials. More recently $CaHPO_4$ has been investigated as protonic conductor [4, 5].

Its structure consists of $CaHPO_4$ chains linked together by Ca-O bonds and three types of hydrogen bonds. Two pairs of PO_4 units are found in each primitive cell. In the P(1)O_4 group the O(2)-P(1)-O(4) angle is smaller than the tetrahedral angle. Two other O-P(1)-O angles, smaller than the tetrahedral one, involve oxygen O(1). In the P(2)O_4 group, P(2)-O(6) and P(2)-O(7) are the longest P-O distances and are sensitively equal, with an average value of 1.547 Å. The only O-P-O angle smaller than 109.5° in the P(2)-O_4 group involves O(6) and O(7). Concerning the three types of hydrogen bonds, one, O(1)-H(2)...O(5), is regular but at the short end of the normal range with O(1)...O(5) = 2.565(1) Å. The second type, O(7)-H(1)...O(7'), is very short with O(7)...O(7') = 2.458(2) Å. H(1) is placed in the centre of symmetry of this bond with O(7)-H(1) = O(7')-H(1) = 1.23 Å and O(7)-H(1)-O(7') = 180° [3]. The third type, O(6)-H(3)...O(8) with O(6)...O(8) = 2.669(1) Å, is in the normal range but is supposed to be statistically disordered with hydrogen covalently bound to half of the O(6) atoms on the average [6, 3]. The ^{31}P MAS-NMR study of the non-annealed compound shows three peaks with proportions 1/2, 1/4 and 1/4, revealing the presence of three types of phosphorus atoms in the structure. The P(1)O_4 group is attributed to the abandoning peak; the other peaks correspond to disordered tetrahedra of P(2) [7]. These results were obtained with the following fit conditions:

(i) The simulation was limited to the isotropic band.

(ii) The deconvolution of the isotropic band was made on the basis of Lorentzian functions.

At high temperature $CaHPO_4$ forms $Ca_2P_2O_7$ in an irreversible chemical process. In this work we study this process by means of X-ray patterns and anisotropic NMR tensors. Thus, a set of samples with different thermal treatments has been prepared. The species were heated in air at atmospheric pressure for 24 h at fixed temperatures ranging between 273 and 723 K. In the NMR investigations we have taken account of the following considerations:

(i) The whole NMR spectra are fitted (isotropic and anisotropic bands).

(ii) All peaks used in the simulation are mixtures of Lorentzian and Gaussian functions. The G/L ratio will be fitted.

0932–0784 / 06 / 0700–0375 $ 06.00 © 2006 Verlag der Zeitschrift für Naturforschung, Tübingen · http://znaturforsch.com

	ZG (MAS)
Pulse length	15.6 μs
Dead time	10 μs
Recycle time	5 s
Resonance frequency	121.49 MHz
MAS spinning speed	8 kHz
Number of scans	720
Number of digitized points	4096
Referencing 0 Hz	H_3PO_4 (85%)

Table 1. Experimental conditions.

Finally, the chemical shift tensor parameters in connection with the crystallographic results on $CaHPO_4$ and $Ca_2P_2O_7$ networks are discussed.

2. Experiment

The alkaline-earth hydrogen phosphate $CaHPO_4$ was obtained by spontaneous reaction at room temperature of a stoichiometric mixture of $Ca(NO_3)_2$ and $NH_4H_2PO_4$ in water in according to

$$\begin{aligned}&Ca(NO_3)_2 + NH_4H_2PO_4\\&\to CaHPO_4 + 2\,NO_3{}^- + NH_4{}^+ + H^+.\end{aligned}$$

The slow evaporation of the solution leads to the formation and precipitation of the compound. The powder was warmed at 353 K for a few hours to eliminate humidity. In order to study the dependence of the thermal decomposition on temperature we have prepared a set of samples at different annealing temperatures. The species were heated in air at atmospheric pressure for 24 h at fixed temperatures ranging between 373 and 723 K.

X-Ray powder diffraction patterns were recorded at a scan step size of 0.017 in 2θ with step time 11.8 s, using a Philips diffractometer operating with copper radiation $K_\alpha = 1.5418$ Å. The unit cell parameters of the samples have been refined by a least square method from the powder data.

The ^{31}P NMR experiments were performed on a Bruker MSL 300 ($B = 7.1$ T) spectrometer working at 121.49 MHz. The powdered samples were pocketed in the rotors and allowed to rotate at a speed of 8 kHz in a Doty MAS probehead. A single $\pi/2$ pulse sequence program (ZG) was used with a pulse length of 15.6 µs. For the recorded spectrum a period of 5 s between successive accumulations was chosen. All chemical shifts δ are given with respect to 85% H_3PO_4, according to the IUPAC convention, i. e. shielding corresponds to negative values. The chemical shift tensor components were obtained using Bruker Winfit software [8]. Specific NMR experimental conditions are reported in Table 1.

3. Results and Discussion

At high temperature, the $MHPO_4$ compounds exhibit an irreversible process consisting of the dehydration-condensation of the monohydrogen phosphate leading to the formation of the diphosphate $P_2O_7^{4-}$. This irreversible process occurs at $T = 723$ K in the case of $CaHPO_4$ [7].

Figure 1 shows the X-ray powder patterns of all species. The X-ray powder diffractograms reveal that the synthesized compound is the anhydrous form of $CaHPO_4$. It crystallizes in the triclinic system (space group $P\bar{1}$) with unit cell parameters: $a = 6.91(1)$ Å, $b = 6.63(3)$ Å, $c = 6.99(3)$ Å, $\alpha = 96.32°$, $\beta = 103.87°$ and $\gamma = 88.37°$, $V = 309.29$ Å^3 which agree well with the literature values [4, 5].

The X-ray powder pattern of the annealed compound at 723 K shows a single phase and confirms the formation of the β-calcium diphosphate (β-$Ca_2P_2O_7$) phase [9]. All the peaks can be indexed in the tetragonal system (space group $P4_1$) with the unit cell parameters $a = 6.68$ Å and $c = 24.20$ Å. However, diffractograms recorded for annealed samples between 300 and 723 K are not indexed due to the existence of two phases ($CaHPO_4$ and β-$Ca_2P_2O_7$).

The ^{31}P NMR spectra for samples rotating at magic angle (MAS) with the frequency $\nu_r = 8$ kHz are shown in Figure 2. We report only the spectra relative to the annealed compound (Fig. 2a) and the species annealed at $T = 573$ K (Fig. 2b) and 723 K (Fig. 2c).

Examination of the crystallographic data shows that H(3) is supposed to be statistically disordered with hydrogen atoms covalently bound to half of the O(6) atoms on the average. Two configurations should, respectively, show H(3) bound to O(6) only and to O(6') only. The two tetrahedra of P(2) and P(2') are inequivalent, so when H(3) links to one of them, the two different groups HPO_4^{2-} and $H_2PO_4{}^-$ are formed in the structure (Fig. 3). In the NMR time scale, the HPO_4^{2-} and $H_2PO_4{}^-$ entities are inequivalent and lead to the appearance of two distinct peaks in the spectrum. Nevertheless, the X-ray diffraction picture is an average one, the H(3) and H(3') sites seem to be simultaneously occupied in the X-ray time scale, leading to a single phosphorus type. To recapitulate, three phosphorus sites exist in the structure with occupancy rate 100% for $P(1)O_4$ and 100% for the disordered site $P(2)O_4$.

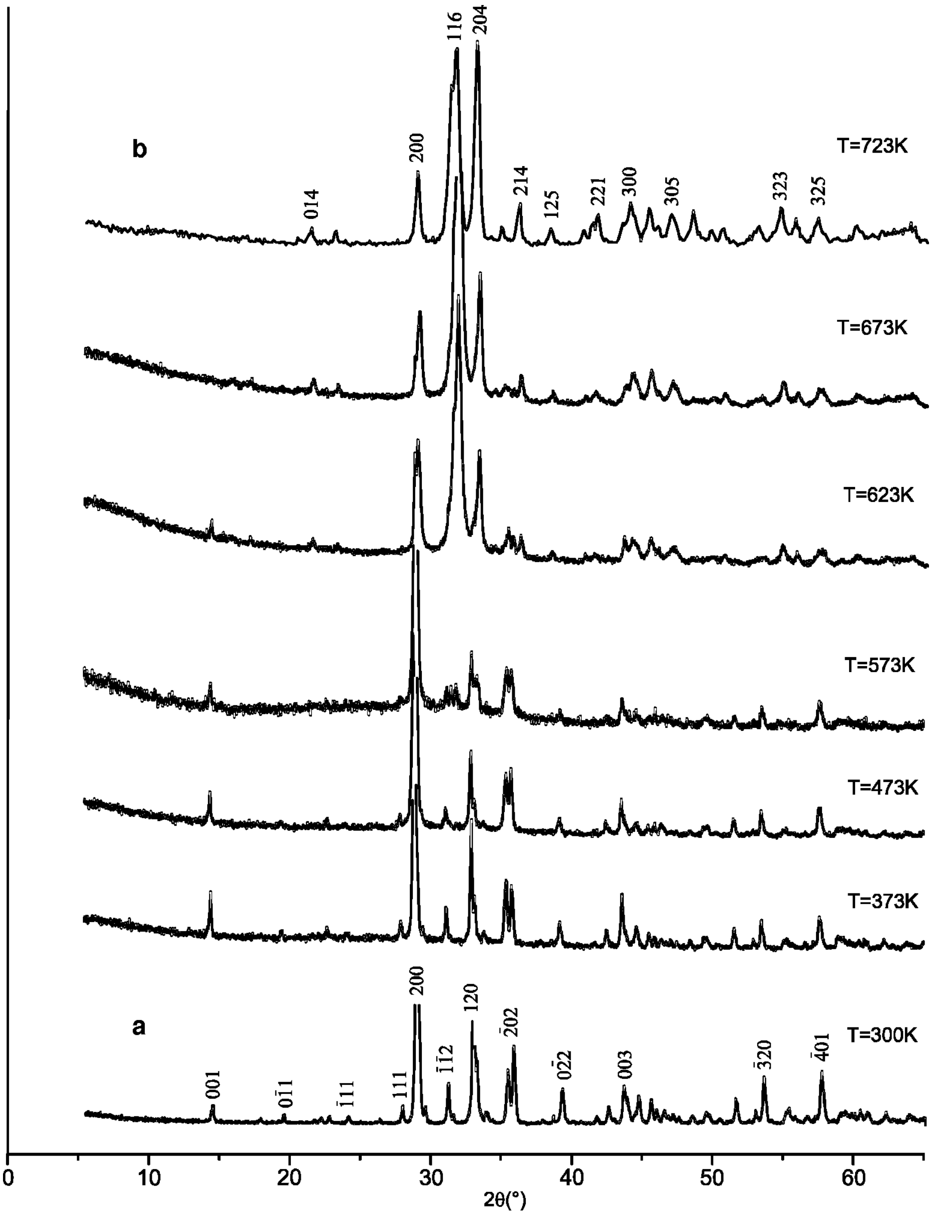

Fig. 1. Powder X-ray patterns of some samples at different temperatures: (a) indexed pattern of $CaHPO_4$; (b) indexed pattern of the sample obtained at 723 K (β-$Ca_2P_2O_7$).

The ^{31}P MAS-NMR study of the non-annealed compound shows three peaks A, B and C at the positions -1.59, -0.36 and 1.26 ppm in the proportions 39, 10 and 51%, respectively, revealing the presence of three types of phosphorus in the structure. The C peak is ascribed to $P(1)O_4$ (site totally occupied); however, the A and B peaks correspond to the disordered site $P(2)O_4$. The ^{31}P MAS-NMR spectrum recorded for the sample annealed at 723 K shows a weak band at 0.46 ppm, confirming the existence of a small amount of $CaHPO_4$ and two intense peaks D and E with equal intensities at -9 and -10.89 ppm which are assigned to the diphosphate species. These results agree with the presence of two types of equally abundant tetrahedra as shown by the X-ray structural determination [9]. The chemical shifts seen for D and E peaks are very close to those

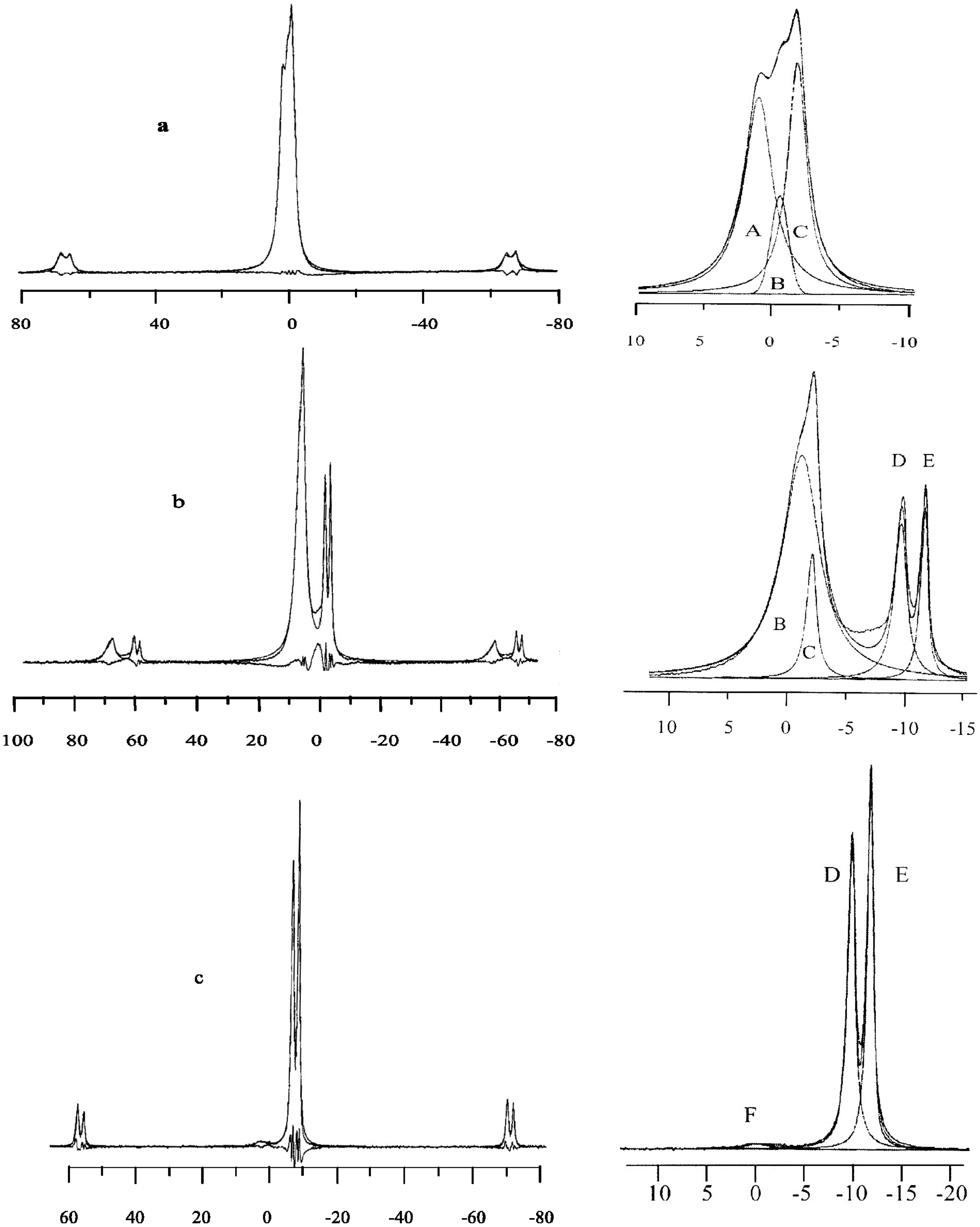

Fig. 2. ^{31}P MAS-NMR spectra of $CaHPO_4$ (a) and annealed species obtained at $T = 573$ K (b) and 723 K (c), $\nu_R = 8$ kHz. Isotropic bands are plotted at the right of each spectrum.

T (K)	g/l	Peaks[a]	% A (esd 1%)	δ_{iso} (ppm)	δ_{cs} (ppm)	FWHM (ppm)	η	δ_{11}	δ_{22}	δ_{33}
298	0	A	51	1.26	−66.0	2.55	0.75	59.0	9.5	−64.8
	1	B	10	−0.36	−33.0	1.50	0.75	28.5	3.8	−33.4
	0	C	39	−1.59	59.4	1.70	0.55	−47.7	−15	57.8
373	0	A	31	1.31	−72.6	2.90	0.65	61.2	14.0	−71.3
	1	B	13	−0.12	−39.6	1.80	0.25	24.6	14.7	−39.7
	0	C	56	−1.49	−59.4	1.78	0.6	46.0	10.4	−60.9
473	0	B	82	−0.55	−52.8	3.56	0.9	49.6	2.1	−53.3
	1	C	9	−1.63	−46.2	1.15	0.95	43.4	−0.5	−47.8
	0	D	9	−8.07	132.0	5.84	0.85	−130.1	−18.0	123.9
573	0	B	63	−0.64	−59.3	3.71	0.35	39.4	18.6	−60.0
	0	C	9	−1.59	52.7	0.97	0.70	−46.4	−9.5	51.4
	0	D	18	−8.90	79.1	1.27	0.95	−86.0	−10.9	70.2
	0	E	10	−10.86	72.5	0.72	0.60	−68.7	−25.4	61.6
673	0	F	16	−4.41	−85.7	10	10	38.4	38.4	−90.0
	0	D	50	−9.00	79.1	1.11	0.85	−82.2	−15.0	70.1
	0.62	E	34	−10.89	72.5	0.88	0.5	−65.3	−29	61.6
723	0	F	2	0.46	*[b]	2.86	*	*	*	*
	0	D	51	−9.00	79.1	0.92	0.9	−84.1	−12.9	70.1
	0	E	47	−10.89	72.5	0.73	0.5	−65.3	−29	61.6

Table 2. ^{31}P NMR parameters for $CaHPO_4$ and annealed species ($\nu_R = 8$ kHz).

[a] A, B, C: relative to $CaHPO_4$; D, E: relative to β-CaP_2O_7; F: relative to $CaHPO_4$ in solid solution.

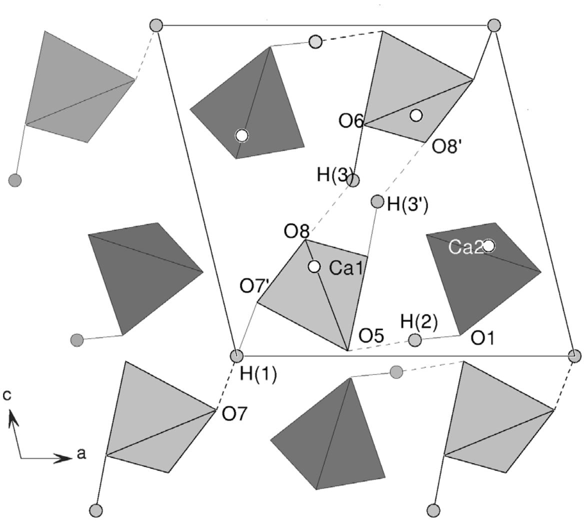

Fig. 3. [010] view of the structure of $CaHPO_4$. Hydrogen bonds are represented by dashed lines, $P(1)O_4$ and $P(2)O_4$ are represented by dark and light gray tetrahedra, respectively.

observed in other diphosphates [10, 11]. The spectra recorded for species obtained at different annealing temperatures ranging between 373 and 723 K show peaks relative to $CaHPO_4$ and β-$Ca_2P_2O_7$ phases. In order to study the dependence of the progress of the thermal decomposition with temperature, the chemical shift tensor is considered.

According to Herzfeld and Berger [12], the parameters of the chemical shift tensors of PO_4 tetrahedra are obtained by an iterative procedure using the Dmfit program [8]. Table 2 presents these results, under the conventional forms δ_{11}, δ_{22} and δ_{33} as well as under the more useful parameters: the isotropic chemical shift δ_{iso}, the chemical shift anisotropy δ_{cs} and the asymmetry parameter η. Because some confusion exists in the literature about the definition of these various parameters, which can lead to misinterpretation, it is necessary to specify the signification of the terms of the Table 2.

δ_{11}, δ_{22} and δ_{33} are the diagonal terms of the chemical shift tensor expressed in the principal axis system (PAS), according to

$$\delta_{11} > \delta_{22} > \delta_{33} \text{ or } \delta_{11} < \delta_{22} < \delta_{33}$$

with the convention that

$$|\delta_{11} - \delta_{22}| < |\delta_{22} - \delta_{33}|, \quad \delta_{iso} = (\delta_{11} + \delta_{22} + \delta_{33})/3,$$
$$\delta_{cs} = \delta_{33} - \delta_{iso}, \quad \text{and } \eta = (\delta_{22} - \delta_{11})/(\delta_{33} - \delta_{iso}).$$

Several empirical models have already been proposed to correlate the different characteristics of the chemical shift with the geometrical properties of the PO_4 tetrahedron [13 – 19].

Un and Klein [13] did establish such type of correlations for PO_4 groups with similar deformations as those observed in phosphate ($CaHPO_4$ and β-$Ca_2P_2O_7$) (Q^0 and Q^1 groups).

The chemical shift tensor orientation is depicted in Fig. 4, where the axes have been renumbered in agreement with the above conventions.

T (K)	$CaHPO_4$			$Ca_2P_2O_7$		
	% $CaHPO_4$ in species	Peaks[a]	% Peaks in $CaHPO_4$	%$Ca_2P_2O_7$ in species	Peaks[a]	% Peaks in $Ca_2P_2O_7$
298	100	A	51	0	D	0
		B	10		E	0
		C	39			
373	100	A	31	0	D	0
		B	13		E	0
		C	56			
473	91	A	0	9	D	100
		B	90		E	0
		C	10			
573	72	A	0	28	D	64
		B	87		E	36
		C	13			
673	16	F	100	84	D	59
					E	41
723	2	F	100	98	D	52
					E	48

Table 3. Phosphorus site occupation in monophosphate ($CaHPO_4$) and diphosphate ($Ca_2P_2O_7$) and their proportions in species obtained at different annealing temperatures.

[a] A, B, C: relative to $CaHPO_4$; D, E: relative to β-CaP_2O_7; F: relative to $CaHPO_4$ in solid solution.

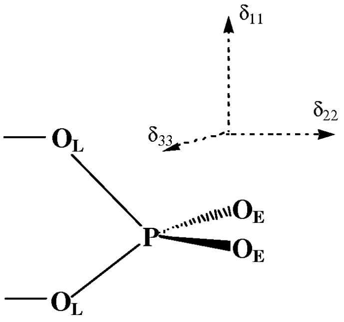

Fig. 4. Chemical shift tensor orientation. Note that (L) and (E) indicate linkage and external oxygen atoms, respectively.

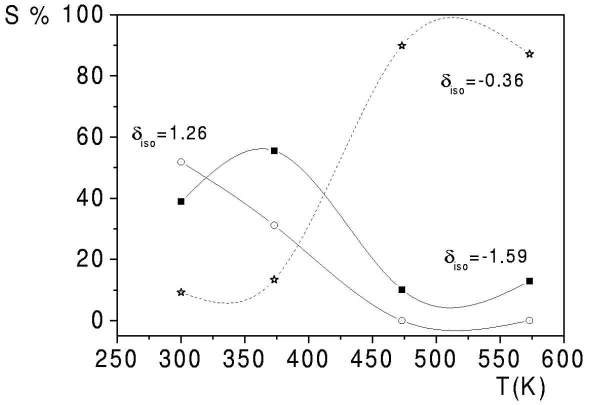

Fig. 5. Abundances of PO_4 tetrahedra in the $CaHPO_4$ phase as a function of the annealing temperature.

When the temperature increases, $CaHPO_4$ exhibits an irreversible chemical process accompanied by a dramatical change in the phosphorus environment due to the formation of the diphosphate $Ca_2P_2O_7$ in accordance with the scheme

$$2HPO_4^{2-} \rightarrow H_2O + P_2O_7^{4-}.$$

In Table 3, we recapitulate the phosphorus site occupation in $CaHPO_4$ and β-CaP_2O_7 at different annealing temperatures. $CaHPO_4$ is polymerized at temperatures greater than 373 K. We note, successively, the polymerization of the more abundant site $P(1)O_4$, the abundant site of disordered $P(2)O_4$ and finally the other site of the last tetrahedron (Fig. 5). The complete polymerization of the $P(1)O_4$ tetrahedron ($\delta_{iso} = 1.26$ ppm) of $CaHPO_4$ is achieved in the vicinity of $T = 450$ K (Fig. 5). The condensation process of $P(1)O_4$ is characterized by regular tensor parameters (Fig. 6a). For temperatures greater than 373 K, the transformation of $P(2)O_4$, deduced from the evolution of the isotropic lines $\delta_{iso} = -0.36$ and $\delta_{iso} = -1.59$ ppm, shows a clear disturbance of tensor parameters (Figs. 6b and c). We note that the variation of δ_{11} and δ_{33} is more important than that of δ_{22}. The δ_{ii} parameters are correlated with the tetrahedra geometry [13]. Indeed, δ_{11} and δ_{33} show an important modification of the geometrical propriety in P-O_L direction, O_L being an atom linkage between P and H atoms. This approach can be reinforced by the chemical process which implies OH groups in the polymerization reaction. The δ_{22} parameter is almost constant and explains that the tetrahedra are slightly distorted in P-O_E liaisons. We deduce that the $CaHPO_4$ network is disturbed above $T = 373$ K. For temperatures greater than 573 K, the $CaHPO_4$ phase is represented by a single isotropic line with irregular position (at 673 and 723 K, $\delta_{iso} = -4.41$ and 0.46 ppm, respec-

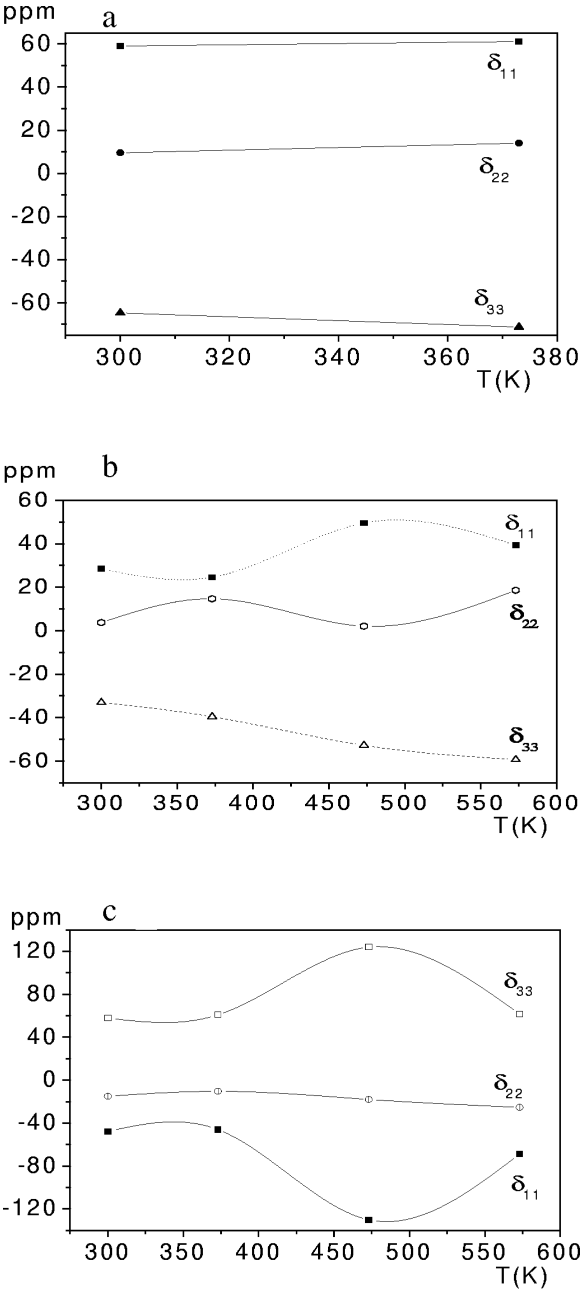

Fig. 6. Variation of the tensor parameters (δ_{11}, δ_{22} and δ_{33}) of peaks observed in $CaHPO_4$: (a) peak A (1.26 ppm); (b) peak B (-0.36 ppm); (c) peak C (-1.49 ppm).

tively). These results show the instability of the PO_4 geometry and environment.

Indeed, at 723 K the X-ray powder pattern shows only the β-$Ca_2P_2O_7$ diffractogram revealing the formation of a solid solution of $CaHPO_4$ in β-$Ca_2P_2O_7$.

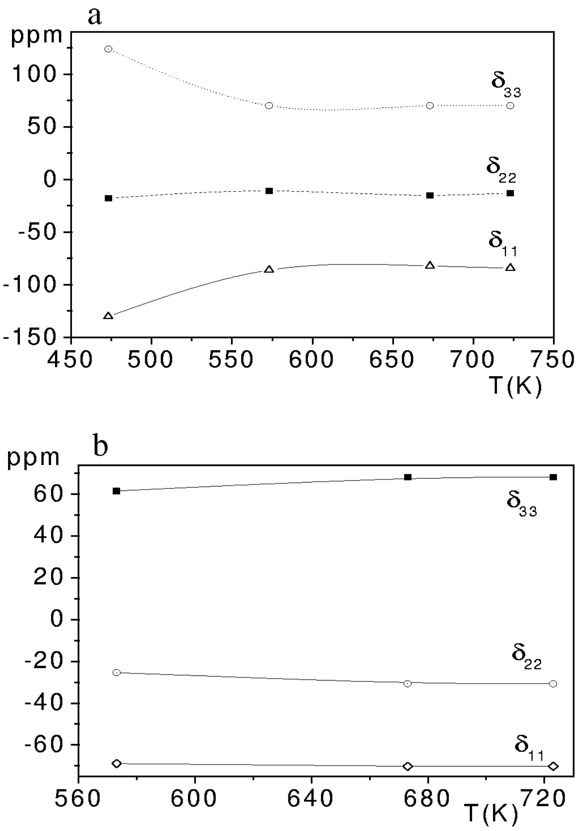

Fig. 7. Variation of the tensor parameters (δ_{11}, δ_{22} and δ_{33}) of peaks observed in β-$Ca_2P_2O_7$: (a) peak D (-8.90 ppm); (b) peak E (-10.86 ppm).

$Ca_2P_2O_7$ appears above 373 K; it is represented by a single band, D ($\delta_{iso} = -8.9$ ppm), in the NMR spectrum, revealing the presence of a unique phosphorus site: the two phosphorus atoms in $P_2O_7^{4-}$ anions are equivalent. The tensor parameters of this peak are disturbed (Fig. 7a), indicating the instability of the $Ca_2P_2O_7$ network. In discordance with the literature results: all $Ca_2P_2O_7$ anhydrous varieties (α-$Ca_2P_2O_7$, β-$Ca_2P_2O_7$ and γ-$Ca_2P_2O_7$) present more than one equivalent phosphorus. Indeed, the X-ray powder pattern shows only the $CaHPO_4$ phase (Fig. 1). These results can be explained by the formation of a solid solution of $Ca_2P_2O_7$ in $CaHPO_4$. From 573 K, the second phosphorus site appears, and the tensor parameters of D and E are regular, confirming the stability of the β-$Ca_2P_2O_7$ network. Above $T = 723$ K, the sample is completely transformed into β-$Ca_2P_2O_7$.

Figures 6 and 7 show a variation of the tensor parameters (δ_{11}, δ_{22} and δ_{33}) of bands observed in $CaHPO_4$ and $Ca_2P_2O_7$, respectively.

The X-ray spectra patterns registered for samples annealed at temperatures ranging from 298 to 473 K represent only peaks relative to the $CaHPO_4$ phase. At 473 K, the amount of $Ca_2P_2O_7$ is about 9%, the X-ray diffractogram relative to $CaHPO_4$ is less resolved with attenuated intensities and large FWHM. Patterns recorded for samples annealed at 573 K and 623 K show peaks relative to $CaHPO_4$ and β-$Ca_2P_2O_7$. In fact, those samples are a mixture of variable amounts, of the indicated compounds. The X-ray diffractogram registered for the species prepared at $T = 673$ K indicates an absence of peaks relative to $CaHPO_4$; however, NMR results show the presence of the $CaHPO_4$ state in an amount of about 16%. We notice that the presence of heterogeneous phases reduces the crystallinity order in the annealed samples. In fact, we note that, when the annealing temperature increases, the X-ray spectra become more resolved. Nevertheless, the spectrum relative to β-$Ca_2P_2O_7$ obtained at 723 K is more resolved than that registered at 673 K, which contains, respectively, 2% and 16% of $CaHPO_4$.

4. Conclusion

$CaHPO_4$ is obtained by spontaneous reaction at room temperature of a stoichiometric mixture of $Ca(NO_3)_2$ and $NH_4H_2PO_4$. At high temperature, $CaHPO_4$ exhibits an irreversible process consisting in the dehydration-condensation of the monohydrogen phosphate, leading to the formation of the diphosphate β-CaP_2O_7. In order to study the dependence of the progress of thermal condensation on temperature, a set of samples has been prepared at different annealing temperatures. The species were heated in air at atmospheric pressure for 24 h at fixed temperatures ranging between 373 to 723 K. All samples were investigated by ^{31}P NMR spectroscopy and X-ray powder diffraction. In the paper reported by Louati et al. [7], authors consider only isotropic bands and fit all ^{31}P NMR peaks with the Lorentzian profile. In the present work, in order to ameliorate the results, we have affined all tensor parameters and considered peaks as a mixture of Lorentzian and Gaussian functions. These studies show clearly that the transformation process $CaHPO_4 \rightarrow CaP_2O_7$ is achieved successively from more to less abundant sites in $CaHPO_4$. The examination of the tensor parameters of phosphorus sites permits us to identify three temperature ranges: 298 – 373 K with regular δ_{ii}, 373 – 450 K with irregular δ_{ii} and $T > 450$ K. Coupled with X-ray technique, it can be concluded that the first temperature range corresponds to a regular lattice of $CaHPO_4$, the second to the formation of a solid solution of $Ca_2P_2O_7$ in $CaHPO_4$ and the third to a solid solution of $CaHPO_4$ in $Ca_2P_2O_7$.

[1] G. R. Sivakumar, E. K. Girija, S. N. Kalkura, and C. Subramanian, Cryst. Res. Technol. **33**, 197 (1998).
[2] J. C. Elliot, D. W. Holcomb, and R. A. Young, Calcif. Tissue Int. **37**, 372 (1985).
[3] A. Boudjada, R. Masse, and J. C. Guttel, Acta Cryst. B **34**, 2692 (1978).
[4] L. Tortet, J. R. Gavarri, G. Nihoul, and A. J. Dianoux, J. Solid State Chem. **132**, 6 (1997).
[5] L. Tortet, J. R. Gavarri, G. Nihoul, and A. J. Dianoux, J. Solid State Ionics **97**, 253 (1997).
[6] B. Dickens, J. S. Bowen, and W. E. Brown, Acta Cryst. B **28**, 797 (1971).
[7] B. Louati, F. Hlel, K. Guidara, and M. Gargouri, J. All. Comp. **394**, 13 (2005).
[8] D. Massiot, H. Theile, and A. Germanius, Bruker Report **43**, 140 (1994).
[9] N. C. Webb, Acta Cryst. **21**, 942 (1966).
[10] N. J. Clayden, S. Esposito, P. Pernice, and A. Aronne, J. Mater. Chem. **11**, 936 (2001).
[11] P. Hartmann, J. Vogel, and B. Schnabel, J. Non-Cryst. Solids **176**, 157 (1994).
[12] J. Herzfeld and A. E. J. Berger, J. Chem. Phys. **73**, 6021 (1980).
[13] S. Un and M. P. Klein, J. Am. Chem. Soc. **111**, 5119 (1989).
[14] D. W. Cruickshank, J. Chem. Soc., 5486 (1961).
[15] J. H. Letcher and J. R. Van Wazer, J. Chem. Phys. **44**, 815 (1966).
[16] A. R. Grimmer, Spectrochim. Acta A **34**, 941 (1978).
[17] A. K. Cheetham, N. J. Clayden, C. M. Dobson, and R. J. B. Jakerman, J. Chem. Soc. Chem. Comm., 195 (1986).
[18] F. Taulelle, T. Loiseau, J. Maquet, J. Livage, and G. Ferey, J. Solid State Chem. **105**, 191 (1993).
[19] G. L. Turner, K. A. Smith, R. J. Kirkpatrick, and E. Oldfield, J. Magn. Reson. **40**, 408 (1986).